ELSEVIER

Journal of Nuclear Materials 277 (2000) 184–198

journal of nuclear materials

www.elsevier.nl/locate/jnucmat

Theory of the late stage of radiolysis of alkali halides

V.I. Dubinko[a], A.A. Turkin[a], D.I. Vainshtein[b], H.W. den Hartog[b,*]

[a] *National Science Center, Kharkov Institute of Physics and Technology, 310108 Kharkov, Ukraine*

[b] *Solid State Physics Laboratory, University of Groningen, Nijenborgh 4, NL-9747 AG Groningen, The Netherlands*

Received 17 February 1999; accepted 30 July 1999

Abstract

Recent results on heavily irradiated natural and synthetic NaCl crystals give evidence for the formation of large vacancy voids, which were not addressed by the conventional Jain–Lidiard model of radiation damage in alkali halides. This model was constructed to describe metal colloids and dislocation loops formed in alkali halides during earlier stages of irradiation. We present a theory based on a new mechanism of dislocation climb, which involves the production of V_F centers (self-trapped hole neighboring a cation vacancy) as a result of the absorption of excess H centers. Voids are shown to arise due to the reaction between F and V_F centers at the surface of halogen bubbles. Critical parameters associated with the bubble-to-void transition are evaluated. Voids can grow to sizes exceeding the mean distance between colloids and bubbles, eventually absorbing them, and, hence, igniting a back reaction between the halogen gas and metal. The amount of radiation damage in alkali halides should be evaluated with account of void formation, which strongly affects the radiation stability of material.

PACS: 61.72.Ji; 61.72.Qq; 61.80.Az

1. Introduction

Irradiation of ionic crystals with electrons of moderate energies (e.g. ~1 MeV) or gamma rays causes electronic excitations that produce Frenkel pairs in only one of the sub-lattices. Consequently, the stabilization of primary point defects in ionic crystals at high temperatures, at which these defects are mobile can be quite distinct from those formed in monoatomic solids such as metals. A well known example of this effect occurs in the alkali halides, where the principal radiation damage consists of *bubbles of fluid halogen* formed by agglomeration of H centers and of the complementary inclusions of alkali metal ('colloids') formed by agglomeration of F centers [1]. Both H and F centers are primary radiation defects in the halide sub-lattice. The H center is a halide interstitial ion with a trapped hole, and an F center is the vacancy in the halide sub-lattice with a trapped electron. There is also evidence [2] that irradiation at low temperatures (where vacancy defects are quite immobile) leads to the formation of numerous *perfect* interstitial dislocation loops. Such perfect loops require both interstitial halogen and interstitial alkali metal: but all previous work showed that ionizing radiation affects principally the halide sub-lattice. The accepted explanation was that a cluster of some small number of halogen molecules formed an interstitial platelet, i.e., a faulted loop, which then 'unfaulted' at a certain size to give the observed perfect loop structures and a corresponding number of dispersed halogen molecular centers [1,2]. In 1977, Jain and Lidiard [3] have formulated a model, according to which, *the dislocation bias* for H centers was the driving force for the colloid growth in alkali halides exactly in the same way as for the *void growth in metals* under irradiation. However, the mechanism of dislocation climb [2] used in the Jain and Lidiard model, requires two H centers and leaves behind *a molecular center*, i.e., halogen molecule in *a stoichiometric vacancy pair* (a stoichiometric vacancy pair consists of two adjacent vacancies, one in the cation

* Corresponding author. Tel.: +31-50 363 4789; fax: +31-50 363 4825.

E-mail address: h.w.den.hartog@phys.rug.nl (H.W. den Hartog).

0022-3115/00/$ - see front matter
PII: S0022-3115(99)00207-X

and one in the anion sub-lattice). Thus, only dislocation loops, dispersed molecular centers and metal colloids were expected to form in the Jain and Lidiard model. One might expect the molecular centers to act as recombination centers for F centers since the energy liberated during the recombination appears to be about 5 eV for NaCl [1]. However, the inclusion of this reaction into the set of rate equations would reduce the steady F concentration such that *colloid growth would be impossible* [1]. Another discrepancy arises when comparing the model with the annealing behavior of irradiated NaCl after irradiation at lower temperatures. Although all traces of color center absorption bands could be removed by annealing at moderate temperatures (e.g., at 250°C), the apparently defect free crystal still persisted in showing a lower density (i.e., a volume expansion) than an unirradiated crystal up to 400°C. Hughes [4] has considered several possible mechanisms for defect back reactions and came to the conclusion that none of them was completely satisfactory. So, the question was: 'Is the simple model of interstitial dislocation loops and dispersed molecular centers adequate at all [4]?' In spite of these problems, the Jain–Lidiard model is still considered to work well in providing a qualitative explanation of the radiation damage in alkali halides. Other approaches to the problem of defect aggregation in irradiated ionic solids, such as the microscopic theory [5] working on an atomic scale, can only describe the early stages of radiolysis, where nucleation of small defect aggregates takes place.

From our results [6–9] obtained for NaCl, which had been irradiated up to fluences 6×10^{22} electrons/m^2 (about 300 Grad or 30 displacements per anion), it follows that large *vacancy voids* (up to hundreds of nm in size) are formed, which cannot be explained by the conventional theory. Below we present a new model of radiation damage formation in alkali halides, which would allow for the creation of halogen bubbles and voids instead of dispersed molecular centers. We will show that, as in metals [10], elastic interaction between inclusions (which can be solid precipitates, gas bubbles or voids) and primary point defects (H and F centers) results in the inclusion bias for absorption of either H or F centers depending on the inclusion size and stress state. The difference between the bias factors of extended defects (ED) of different kinds or sizes will be shown to be the main driving force of the microstructural evolution under irradiation.

The paper is organized as follows. In Section 2, we discuss a mechanism of the production of V_F centers due to the absorption of H centers by edge dislocations, which represents a new mechanism of dislocation climb. The driving force of the climb is the dislocation bias towards absorption of H centers due to stronger elastic interaction with H centers as compared to F centers. In Section 3, we analyze the bias factors of colloids, bubbles and voids arising due to a difference in their elastic interaction with H and F centers. In Section 4, the rate equations for the primary and secondary point defects (PD) are presented. In Section 5, we will derive a set of equations for growth rates of ED determined by the difference in their bias factors, consider the asymptotic solutions and find the critical parameters that control the transition of some of the halogen bubbles to rapidly growing voids. In Section 6 we consider simultaneous evolution of all ED present in the system, and find the dependence of their mean sizes and number densities on the irradiation dose at a fixed temperature and dislocation density. The temperature dependence of the ED evolution is considered in Section 7. The results are discussed and compared with experimental data on radiation damage in NaCl in Section 8, and summarized in Section 9.

2. Model of dislocation climb

When a H center approaches a dislocation, it is assumed to displace a lattice cation and form with this ion a stoichiometric interstitial pair (needed for the dislocation climb) *leaving behind a hole trapped by a cation vacancy* (see Fig. 1). The latter is known as the V_F center, which is a mobile 'antimorph' of the F center (electron trapped in an anion vacancy). The new reaction requires only one H center as compared to two H centers meeting at the dislocation core, according to the existing mechanism [2]. This is a rather improbable event during irradiation at elevated temperatures, where F centers are mobile as well, and their fluxes to dislocations differ from H center fluxes only due to the dislocation bias. The proposed reaction is more

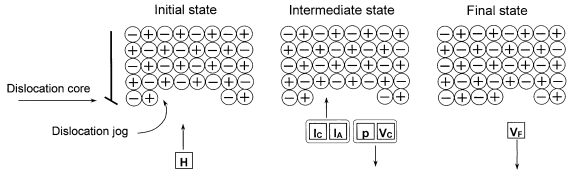

Fig. 1. Production of the V_F center as a result of absorption of a H center by an edge dislocation. When a H center approaches the dislocation, it displaces a lattice cation and forms with it a stoichiometric interstitial pair, $i_A + i_C$, where i_A and i_C are the anion and cation interstitials, respectively and a H center is $i_A + p$ (i.e., an interstitial anion plus a hole, p). A cation vacancy, V_C , and a hole, are produced in the same reaction. The interstitial pair joins a dislocation jog leaving behind the hole trapped at the cation vacancy, that is a V_F center. The recombination reaction of the V_F center with a F center produces a vacancy pair that restores the previous state of the dislocation. So, the production of V_F centers requires a bias of dislocations for H centers.

straightforward, and it should be energetically favorable since the formation energy of V_F center is much less than that of H center. However, this question needs more detailed theoretical consideration, which is in progress.

As far as the dispersed halogen molecules are concerned, they can be produced in our case as well. Indeed, mobile V_F centers can subsequently recombine with each other to form a halogen molecule sitting in a double vacancy pair (i.e., in two adjacent stoichiometric vacancy pairs). This can be a nucleus of a halogen bubble that is formed by a subsequent absorption of H centers as described in Section 5.

But what is more important is that the V_F center is the antimorph of the F center so that their mutual recombination would result in production of a stoichiometric vacancy pair (in both anion and cation sublattices). Such a recombination is expected to take place first of all at halogen bubble surfaces since coherent colloids are assumed to be transparent for V_F centers and do not trap them. Indeed, the V_F center is a defect in the cation sub-lattice that is not damaged by coherent colloids.[1]

An important consideration is that the production of V_F centers by dislocations requires excess of incoming H centers over F centers, since the latter induce a back reaction (Fig. 1). Similarly, the production of vacancy pairs at the bubble surface requires an excess of incoming F centers over H centers. This means that all reactions involved in the production and absorption of V_F centers at extended defects are controlled by the biases for absorption of H centers or F centers.

An edge dislocation is biased towards absorption of H centers due to stronger elastic interaction with them as compared to F centers. So dislocations are a potential source of extra F centers and V_F centers under irradiation. But this potential can be realized provided there are other extended defects with lower (or negative) bias for H centers that could be the sinks for the extra F centers. The dislocation bias is determined by the ratio of relaxation volumes associated with H and F centers, Ω_H/Ω_F, and is given by [10]

$$\delta_d = \ln\left(\frac{\Omega_H}{|\Omega_F|}\right)\Big/\ln\left(\frac{2}{L_H k_H}\right), \qquad L_H = \frac{\mu b(1+\nu)}{3\pi KT(1-\nu)}\Omega_H, \tag{1}$$

where b is the host lattice spacing, μ the shear modulus of the matrix, ν the Poisson's ratio, k_H the square root of the total sink strength of all ED for H centers, and kT has its usual meaning. In the following section we consider the biases of other ED modeled as spherical inclusions in an elastic medium.

[1] Accumulation of vacancy pairs at incoherent colloids was considered in the previous papers [8,9].

3. Bias of spherical inclusions due to elastic interaction difference (EID)

A bias of a sink for absorption of PD of a certain type is given by the difference between the sink efficiencies to capture defects of opposite signs (H and F centers in the case under consideration). Since irradiation produces equal numbers of H and F centers, the radiation-induced growth (or shrinkage) rate of each sink is directly proportional to the difference between its bias and the mean bias of the system. The derivation of sink efficiencies, Z^S, involves the solution of the diffusion problem in the sink region of influence with consideration of its elastic interaction with PD both in equilibrium and in the saddle point configurations. As was summarized in Refs. [10,11], the former determines the image (im) [12], the modulus (μ) [13] and elastic anisotropy (ea) [14] modes of interaction between a sink and PD modeled as spherical inclusions in an elastic medium. On the other hand, the diffusion parameters of PD are those in saddle points for diffusion jumps, which are also affected by the stress field of the sink. The immediate consequence of this is the stress-induced anisotropy of PD near the sink, which influences its capture efficiency [15–17]. If each of these effects causes a small correction to Z^S, then the resulting expression for a capture efficiency of a sink of the radius R can be obtained approximately by summation of all corresponding corrections, which are to be evaluated separately, as has been done for metals in Refs. [10,11]

$$Z_n^S = 1 + \Delta Z_n^{im} + \Delta Z_n^{\mu} + \Delta Z_n^{ea} + \Delta Z_n^{ed}, \quad n = H, F, \tag{2}$$

where the subscripts determine the PD type, and the superscript in Z^S determines the sink type, while the ΔZ values correspond to the above mentioned effects and are given by the following formulas:

$$\Delta Z_n^{im} = \frac{\alpha_n^{im} b}{R}, \quad \alpha_n^{im} = \left[\frac{(\mu-\mu_C)(1+\nu)^2\Omega_n^2}{36kT(1-\nu)}\right]^{1/3}, \tag{3}$$

$$\Delta Z_n^{\mu} = -\frac{3}{56}\frac{\alpha_n^{\mu}}{kT\mu^2}(\sigma_{rr})^2, \tag{4}$$

$$\Delta Z_n^{ea} = -1.7\times 10^{-3}\xi^2\left(\frac{1+\nu}{1-2\nu}\right)^2\left(\frac{\Omega_n\sigma_{rr}}{kT}\right)^2, \tag{5}$$

$$\Delta Z_n^{ed} = \alpha_n^d\frac{\sigma_{rr}}{\mu}, \quad \alpha_n^d = -\left(5d_n^{(2)} + 2d_n^{(3)}\right)/40, \tag{6}$$

where μ_C is the shear modulus of the inclusion, Ω_n the point defect relaxation volume, α_n^{μ} the PD polarizability,

σ_{rr} the normal stress at the inclusion boundary, $d_n^{(2)}$ and $d_n^{(3)}$ the independent components of the 'elastodiffusion tensor' [17], and ξ is the elastic anisotropy parameter.

The inclusion bias for H centers, δ_s, is given by the difference $(Z_H^s/Z_F^s) - 1$:

$$Z_F^s \delta_s(R, \sigma_{rr}) = \alpha^{im}(b/R) + \alpha^d(\sigma_{rr}/\mu) + \alpha^{\mu,\xi}(\sigma_{rr}/\mu)^2, \quad (7)$$

$$\alpha^{im} = \left(\alpha_H^{im} - \alpha_F^{im}\right)/b, \quad \alpha^d = \left(\alpha_H^d - \alpha_F^d\right), \quad (8)$$

$$\alpha^{\mu,\xi} = \frac{3}{56kT}(\alpha_v^\mu - \alpha_i^\mu) - 1.7 \times 10^{-3}\left(\frac{1+v}{1-2v}\right)^2\left(\frac{\mu\xi}{kT}\right)^2(\Omega_i^2 - \Omega_v^2), \quad (9)$$

where a factor Z_F^s in most cases is close to unity, and the dimensionless bias constants, α, are defined to be positive as shown in Table 1. It can be seen that δ_s depends on the inclusion radius and stress state that is different for colloids, gas bubbles and voids. They are considered in detail below.

3.1. Colloid bias

Below the melting temperature, metallic colloids can be in two principally different states. Since the colloids are formed by F centers they are expected to be coherent with the host matrix as long as they are small. In this, coherent, state, there exists a misfit, ε, which is equal to the difference between the lattice constants of the colloid and that of the host lattice. Positive (or negative) misfit means that colloid is under compressive (or tensile) stress given by $\sigma_{rr} = \sigma_\varepsilon$

$$\sigma_\varepsilon = -\frac{3K_C\varepsilon}{1 + 3K_C/4\mu}, \quad (10)$$

where K_C is the colloid bulk modulus. The misfit energy increases with increasing colloid radius, which favors energetically the loss of coherency at some threshold radius, R_C^{th}, and leads to a transition to the incoherent state. The value of R_C^{th} can be estimated from the balance between the misfit energy gained in the process and the energy of the dislocation loop needed to compensate for the change of the colloid volume and the difference in surface energies of coherent and incoherent colloids, γ_{in} and γ_c

$$R_C^{th} \approx \frac{\mu b \ln(8R_C^{th}/er_d)/2\pi(1-v) + 2(\gamma_{in} - \gamma_c)}{\sigma_\varepsilon}, \quad (11)$$

where r_d is the dislocation core radius. Consequently, the biases of the two colloid types are different. The first is given by

$$\delta_{coh} = \alpha_c^{im} b/R_C + \delta_\varepsilon, \quad \delta_\varepsilon = \alpha^d(\sigma_\varepsilon/\mu) + \alpha^{\mu,\xi}(\sigma_\varepsilon/\mu)^2, \quad (12)$$

where δ_ε is the constant misfit bias, and α_c^{im} is the constant of the image interaction for coherent colloids,

Table 1
Material parameters of NaCl and Na colloids used in calculations

Parameter	Value
Irradiation temperature, T (K)	373
Dose rate, K, Mrad/h (dpa/s)	240 (6.7×10^{-6})
Maximum dose, Grad (dpa)	1000 (100)
Dislocation density, ρ (m^{-2})	10^{14}
Diffusion coefficient of H-centers, D_H ($m^2\ s^{-1}$)	$10^{-6}\exp(-0.1\ eV/kT)$
Diffusion coefficient of F-centers, D_F ($m^2\ s^{-1}$)	$10^{-6}\exp(-0.8\ eV/kT)$
Diffusion coefficient of V_F centers, D_v ($m^2\ s^{-1}$)	$10^{-6}\exp(-0.69\ eV/kT)$
Formation energy of F centers, E_F^f (eV)	0.9
F–H recombination rate constant, β_r (m^{-2})	10^{20}
Matrix shear modulus, μ (GPa)	15
Coherent colloid shear modulus, μ_C (GPa)	10
Interface energy of coherent colloid, γ_c (J/m^2)	0.01
Interface energy of incoherent colloid, γ_{in} (J/m^2)	1.07
Surface energy of NaCl, γ (J/m^2)	0.82
Atomic volume of the host lattice, ω (m^{-3})	4.4×10^{-29}
Ratio of relaxation volumes of H and F centers, $\Omega_H/\lvert\Omega_F\rvert$	5
Dislocation bias, δ_d	0.7
Colloid misfit, ε	0.06
Misfit bias, δ_ε	0.55
Elastic-diffusion anisotropy interaction constant, α^d	4
'Image' interaction constant for coherent colloids, α_c^{im}	0.34
Image interaction constant for incoherent colloids and voids, α^{im}	1.97
Modulus minus elastic anisotropy interaction constant, $\alpha^{\mu,\zeta}$	0

which is expected to be less than that for incoherent colloids and voids, $\alpha^{\rm im}$ (see Table 1).

The incoherent colloid bias is inversely proportional to its size

$$\delta_{\rm in}(R_{\rm C}) \approx \left(\alpha^{\rm im} + \frac{\alpha^{\rm d} 2\gamma_{\rm in}}{\mu b}\right)\frac{b}{R_{\rm C}} + \frac{\alpha^{\mu,\xi}}{\mu^2}\left(\frac{2\gamma_{\rm in}}{R_{\rm C}}\right)^2. \tag{13}$$

In NaCl, considered below in more detail, coherent sodium colloids have a negative misfit (about 7% for fcc- and 4% for bcc-lattices), and hence a positive misfit bias, which means that they can form only if the dislocation bias is larger than δ_ε.

3.2. The bias of halogen bubbles and vacancy voids

The normal stress at the bubble surface is given by the difference between its surface tension and the gas pressure, $P : \sigma_{rr} = 2\gamma/R_{\rm B} - P$, where γ is the surface free energy of a bubble. Accordingly, its bias takes the form

$$\delta_{\rm B}(R_{\rm B}, P) \approx \alpha^{\rm im}\frac{b}{R_{\rm B}} + \frac{\alpha^{\rm d}}{\mu}\left(\frac{2\gamma}{R_{\rm B}} - P\right) + \frac{\alpha^{\mu,\xi}}{\mu^2}\left(\frac{2\gamma}{R_{\rm B}} - P\right)^2, \tag{14}$$

whence it follows that it has a negative constituent proportional to the gas pressure, which will be shown to play a critical role in the void formation.

For voids we have $P \ll 2\gamma/R$, and so their bias decreases steadily with increasing size similar to that of incoherent colloids

$$\delta_{\rm V}(R_{\rm V}) \approx \left(\alpha^{\rm im} + \frac{\alpha^{\rm d} 2\gamma}{\mu b}\right)\frac{b}{R_{\rm V}} + \frac{\alpha^{\mu,\xi}}{\mu^2}\left(\frac{2\gamma}{R_{\rm V}}\right)^2. \tag{15}$$

Accordingly, voids can grow if their size exceeds a critical one determined by the mean bias and the void bias constants. Below this size, voids would capture more H centers than F centers, which would fill it with gas.

4. Rate equations for point defects

In this paper, we will concentrate at the temperature range, in which all PD are mobile but their thermal emission from ED is yet negligibly small as compared to the production by irradiation. In this range, the mean concentrations of primary PD, $\bar{c}_{\rm F,H}$ are determined by the rate equations

$$\frac{{\rm d}\bar{c}_{\rm F,H}}{{\rm d}t} = K - k^2_{\rm F,H} D_{\rm F,H}\bar{c}_{\rm F,H} - \beta_{\rm r}(D_{\rm F} + D_{\rm H})\bar{c}_{\rm F}\bar{c}_{\rm H}, \tag{16}$$

$$k^2_{\rm F,H} = Z^{\rm d}_{\rm F,H}\rho_{\rm d} + Z^{C}_{\rm F,H} 4\pi N_{\rm C}\overline{R}_{\rm C} + Z^{\rm B}_{\rm F,H} 4\pi N_{\rm B}\overline{R}_{\rm B} + Z^{\rm V}_{\rm F,H} 4\pi N_{\rm V}\overline{R}_{\rm V}, \tag{17}$$

where K is the generation rate of F and H centers, $k^2_{\rm F,H}$ the sink strengths associated with absorption by ED, $\beta_{\rm r}$ the constant of their bulk recombination, $\rho_{\rm d}$ the dislocation density, $N_{\rm S}$ the number density of S-type EDs, and $\bar{R}_{\rm S}$ is the mean radius.

The concentration of V_F centers is determined by their production at dislocations, the bulk recombination and absorption by voids

$$\frac{{\rm d}\bar{c}_v}{{\rm d}t} = K_v - k_v^2 D_v \bar{c}_v - \beta_r (D_v + D_v)\bar{c}_v^2, \tag{18}$$

$$K_v = \left(Z^{\rm d}_{\rm H} D_{\rm H}\bar{c}_{\rm H} - Z^{\rm d}_{\rm F} D_{\rm F}\bar{c}_{\rm F}\right)\rho_{\rm d}, \quad k_v^2 = 4\pi N_{\rm V}\overline{R}_{\rm V}. \tag{19}$$

We are interested in the steady-state solutions so that $d\bar{c}_n/dt = 0$, and PD concentrations are connected by a simple relation

$$D_{\rm F}\bar{c}_{\rm F} = D_{\rm H}\bar{c}_{\rm H}\left(k^2_{\rm H}/k^2_{\rm F}\right). \tag{20}$$

Substituting Eq. (20) into Eq. (19) and performing some algebraic operations we obtain that the V_F center source is proportional to the difference between the dislocation bias, $\delta_{\rm d}$, and the mean bias of all ED, $\bar{\delta}$

$$K_v = D_{\rm H}\bar{c}_{\rm H} Z^{\rm d}_{\rm F}\rho_{\rm d}\left(\delta_{\rm d} - \bar{\delta}\right), \quad \delta_{\rm d} = \frac{Z^{\rm d}_{\rm H} - Z^{\rm d}_{\rm F}}{Z^{\rm d}_{\rm F}}, \quad \bar{\delta} = \frac{k^2_{\rm H} - k^2_{\rm F}}{k^2_{\rm F}}. \tag{21}$$

5. Nucleation and growth of extended defects

5.1. Colloids

The colloid growth (or shrinkage) rate is given by the difference of F and H center influxes, or equivalently, by the difference between the mean bias and the colloid bias that depends on its size and structure/aggregation state

$$\frac{{\rm d}R_{\rm C}}{{\rm d}t} = \frac{1}{R_{\rm C}}\left[Z^{\rm C}_{\rm F} D_{\rm F}\bar{c}_{\rm F} - Z^{\rm C}_{\rm H} D_{\rm H}\bar{c}_{\rm H}\right] = \frac{1}{R_{\rm C}} Z^{\rm C}_{\rm F} D_{\rm H}\bar{c}_{\rm H}\left(\bar{\delta} - \delta_{\rm C}\right). \tag{22}$$

Accordingly, the colloid growth rate is negative below some critical radius, $R^{\rm crit}_{\rm C} = \alpha^{\rm im} b/(\bar{\delta} - \delta_\varepsilon)$, which determines the nucleation barrier and, hence, the nucleation rate of colloids.

We will consider the stage after the nucleation is over. At this stage, the final number density of colloids does not depend on the nucleation rate, but it is determined by the mechanism of the radiation induced coarsening (RIC). The RIC mechanism was proposed [12] to determine the late stage evolution of voids under irradiation of metals in the same way as the Ostwald ripening mechanism determines thermal aging of precipitates. However, the RIC mechanism has a purely kinetic origin being the result of the inversely propor-

tional dependence of void bias for interstitial absorption on the void radius. The colloid bias has practically the same dependence, since a constant constituent from the misfit does not influence the competition between colloids of different sizes but limits an overall supply of extra F centers coming from other ED. So an asymptotic in-time solution for the number density of colloids can be found to depend on the difference between the biases of other sinks and the mean bias

$$N_C = \frac{\sum_{S\neq C} k_S^2(\delta_S - \bar{\delta})}{2\pi\alpha_c^{im} b}. \tag{23}$$

In this regime, the mean radius of colloids is completely determined by their bias constant, α_c^{im}, and by the irradiation and material parameters (via the mean concentration of H centers)

$$\frac{d\overline{R}_C}{dt} = \frac{\alpha_c^{im} b}{2\overline{R}_C^2} D_H \bar{c}_H. \tag{24}$$

Accordingly, the rate of growth of the colloid volume fraction is given by

$$\frac{dV_C}{dt} = \sum_{S\neq C} k_S^2 \left(\delta_S - \bar{\delta}\right) D_H \bar{c}_H. \tag{25}$$

5.2. Bubbles

Nucleation of halogen bubbles can start as the result of recombination of V_F centers, the rate of which is proportional to the square of V_F center concentration. The steady-state concentration of point defects is inversely proportional to their mobility. The mobility of V_F centers is close to that of F centers (their migration activation energies are 0.7 and 0.8 eV, respectively), which is much lower than the mobility of H centers having migration energy of 0.1 eV. Accordingly, the recombination of V_F centers is much stronger than that of H centers and is more likely to provide immobile molecular centers in pure crystal. In real crystals, however, impurity ions can act as traps for H centers and provide nucleation sites. When several H centers come to such a site they combine to form a halogen bubble which 'digs its own hole in the lattice by displacing a lattice cation and a neighboring lattice anion on to the edge of the dislocation loop' [1]. This process is exactly analogous to the loop punching by growing helium bubbles in metals [18,19]. The threshold pressure for the loop punching is inversely proportional to the bubble radius [18,20]: $\sigma_{rr}^{th} \approx -(\mu b + 2\gamma)/R_B$. Substituting it into Eq. (14) we obtain a simple dependence of the bubble bias on the radius

$$\delta_B(R) \approx \frac{\alpha^{im} b}{R} - \alpha^d \frac{b}{R} + \alpha^{\mu,\xi}\left(\frac{b}{R}\right)^2, \tag{26}$$

from which it follows that a small halogen bubble, $R < R^{th}$, has a higher bias for H centers than the mean bias, and so it can absorb extra H centers and grow via SIA-loop punching, which can be an *additional driving force* for the separation of the H and F centers into bubbles and metal colloids

$$R^{th} = b\left(-\frac{1}{2}\frac{\alpha^d - \alpha^{im}}{\bar{\delta}} + \sqrt{\frac{1}{4}\left(\frac{\alpha^d - \alpha^{im}}{\bar{\delta}}\right)^2 + \frac{\alpha^{\mu,\xi}}{\bar{\delta}}}\right). \tag{27}$$

At $R > R^{th}$, extra F centers start to arrive at the bubble surface and recombine with V_F centers producing stoichiometric vacancy pairs that would increase the bubble size and so decrease the pressure below the threshold level for loop punching. After that, the bubble pressure is determined both by the number of halogen molecules and the number of vacancy pairs in it via the equation of state. Accordingly, the bubble evolution takes place in the two-dimensional phase space of the number of halogen molecules, n_{Gas}, and the number of vacancy pairs in it, $n_{Vac} = 4\pi R_B^3/\omega$, where ω is the molecular volume of the host NaCl lattice. The first one increases if $\delta_B > \bar{\delta}$ while the second one increases in the opposite case of $\delta_B < \bar{\delta}$, such as follows:

$$\frac{dn_{Gas}}{dt} = 2\pi R_B Z_F^B D_H \bar{c}_H \left[\delta_B(n_{Vac}, n_{Gas}) - \bar{\delta}\right] \Theta\left(\delta_B - \bar{\delta}\right),$$
$$\Theta(x) \equiv \begin{cases} 1, & x > 0, \\ 0, & x \leqslant 0, \end{cases} \tag{28}$$

$$\frac{dn_{Vac}}{dt} = 4\pi R_B Z_F^B D_H \bar{c}_H \left[\bar{\delta} - \delta_B(n_{Vac}, n_{Gas})\right] \Theta\left(\bar{\delta} - \delta_B\right), \tag{29}$$

where the dependence $\delta_B(n_{Vac}, n_{Gas})$ can be found from Eq. (14) using the appropriate equation of gas state such as the modified Van der Waals gas law

$$P(n_{Vac}, n_{Gas}) = n_{Gas} kT/(n_{Vac}\omega - n_{Gas}\omega_{Gas}), \tag{30}$$

where ω_{Gas} is the effective volume occupied by one halogen molecule in the bubble.

Now, Eqs. (28) and (29) are the components of the vector of the bubble motion rate in the n_{Gas}, n_{Vac} phase space that are schematically shown in Fig. 2. Below some critical number of halogen molecules, a bubble is forced to occupy a stable position along the curve in the 'valley' where both components of the bubble growth rate are zero. A gradual decrease of the mean bias, which is due to the colloid growth, makes the bubbles move adiabatically along the curve until they reach a critical point, beyond which n_{Vac} would increase inexorably at n_{Gas} remaining constant. Thus a conversion of bubbles to voids would take place after some threshold irradiation dose. Below that dose, bubbles are

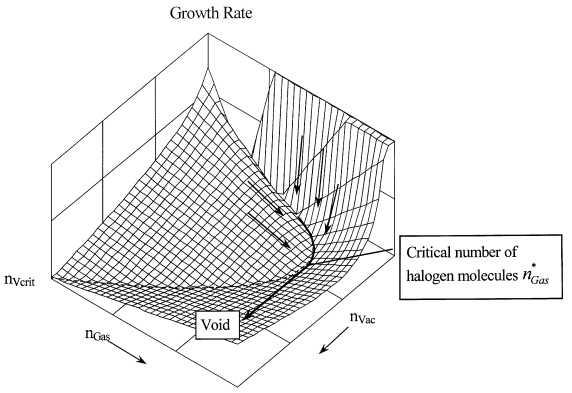

Fig. 2. The evolution path of bubbles resulting in their conversion to voids. Below the critical number of halogen molecules, n^*_{Gas}, the bubbles move slowly along the valley, which provide the only stable path towards the point where the critical number of halogen molecules is reached. After the point is reached, the number of vacancies starts to increase, while the number of gas molecules stays constant. n_{Vcrit} is the critical number of vacancies required for growth of an empty void ($n_{\mathrm{Gas}} = 0$).

in a quasi-steady state with their bias equal to the mean bias of the system. The total number of halogen molecules in bubbles and their volume fraction increases steadily with increasing colloid volume fraction, and is given by the balance between the amounts of halogen molecules in bubbles and metal atoms in colloids

$$N_{\mathrm{Gas}}(t) = \frac{1}{2\omega} V_{\mathrm{C}}(t), \quad V_{\mathrm{B}}(t) \approx \frac{\omega_{\mathrm{Gas}}}{2\omega} V_{\mathrm{C}}(t). \tag{31}$$

So to find the mean number of halogen molecules in one bubble, $\bar{n}_{\mathrm{Gas}}$, one should know the bubble number density. A homogeneous nucleation from the recombination of V_F centers would result in the final concentration of bubbles, ωN^0_{B}, close to the maximum steady-state concentration of V_F centers, which can be easily estimated from Eq. (18) as follows:

$$\omega N^0_{\mathrm{B}} \approx \sqrt{K_v/D_v\beta} N_{\mathrm{B}} = \eta N^0_{\mathrm{B}}. \tag{32}$$

Impurities can either facilitate or hamper the nucleation process, which will be taken into account by a factor η so that $N_{\mathrm{B}} = \eta N^0_{\mathrm{B}}$ and $\bar{n}_{\mathrm{Gas}} = N_{\mathrm{Gas}}/N_{\mathrm{B}}$.

5.3. Critical parameters controlling bubble-void transition

The critical number of halogen molecules required for the bubble-void transition, n^*_{Gas}, corresponds to the condition that Eq. (29) has no roots, i.e., $\mathrm{d}n_{\mathrm{Vac}}/\mathrm{d}t > 0$ at any n_{Vac}. The mathematical procedure is exactly the same as that used to find a critical umber of gas atoms for the bubble-void transition in metals [21,10]. In the case when radiation-induced PD dominate over thermal PD, one has in the linear approximation in stress ($\alpha^{\mu,\xi} = 0$) [10]

$$n^*_{\mathrm{Gas}} = \frac{8\pi\gamma_K R^2_{\mathrm{Vcrit}}(1+\varepsilon)^2}{kT(2+\varepsilon)^4}, \quad R_{\mathrm{Vcrit}} = \frac{2\gamma_K}{\sigma_K}, \tag{33}$$

$$\varepsilon = (1+3\varphi)^{1/2}, \quad \varphi = \sigma_K \omega_{\mathrm{Gas}}/kT, \tag{34}$$

$$\gamma_K = \gamma + \mu b \frac{\alpha^{\mathrm{im}}}{2\alpha^{\mathrm{d}}}, \quad \sigma_K = \mu \frac{\bar{\delta}}{\alpha^{\mathrm{d}}}, \tag{35}$$

where R_{Vcrit} is the critical radius for the vacancy void growth (at $n_{\mathrm{Gas}} = 0$), γ_K and σ_K are the effective parameters, which play the same role as the surface energy and tensile external stress that can induce void formation from thermal vacancies without irradiation [10].

5.4. Vacancy voids

The gas pressure in the growing void drops very rapidly as compared to the surface tension value, and the void growth rate is determined by the excess F center flux

$$\frac{\mathrm{d}R_{\mathrm{V}}}{\mathrm{d}t} = \frac{1}{R_{\mathrm{V}}}\left(Z^{\mathrm{V}}_{\mathrm{F}} D_{\mathrm{F}} \bar{c}_{\mathrm{F}} - Z^{\mathrm{V}}_{\mathrm{H}} D_{\mathrm{H}} \bar{c}_{\mathrm{H}}\right) = \frac{1}{R_{\mathrm{V}}} Z^{\mathrm{V}}_{\mathrm{F}} D_{\mathrm{H}} \bar{c}_{\mathrm{H}} \left(\bar{\delta} - \delta^{\mathrm{eff}}_{\mathrm{V}}\right), \tag{36}$$

where $\delta^{\mathrm{eff}}_{\mathrm{V}}$ is equal to δ_{V} defined by Eq. (15) provided that there are sufficient V_F centers available for the recombination with extra F centers to produce stoichiometric vacancy pairs. In the opposite case, a flux of V_F centers is a limiting factor of the void growth, which is then given by

$$\frac{\mathrm{d}R_{\mathrm{V}}}{\mathrm{d}t} = \frac{1}{R_{\mathrm{V}}} Z^{\mathrm{V}}_{v} D_v \bar{c}_v. \tag{37}$$

It is possible to describe both these regimes by Eq. (36), by defining the following expression for the effective void bias that takes into account both V_F and F center fluxes and depends on the sink strengths and biases:

$$\delta^{\mathrm{eff}}_{\mathrm{V}}(R_{\mathrm{V}}, k^2_{\mathrm{S}}) = \begin{cases} \delta_{\mathrm{V}}(R_{\mathrm{V}}) & \text{if } \delta_{\mathrm{V}}(R_{\mathrm{V}}) > \delta_{\mathrm{VS}}(k^2_{\mathrm{S}}), \\ \delta_{\mathrm{VS}}(k^2_{\mathrm{S}}) & \text{if } \delta_{\mathrm{V}}(R_{\mathrm{V}}) < \delta_{\mathrm{VS}}(k^2_{\mathrm{S}}), \end{cases} \tag{38}$$

$$\delta_{\mathrm{VS}}(k^2_{\mathrm{S}}) = \langle \delta_{\mathrm{C}}(R_{\mathrm{C}}) \rangle + \frac{k^2_{\mathrm{d}}}{k^2_{\mathrm{V}}} (\langle \delta_{\mathrm{C}}(R_{\mathrm{C}}) \rangle - \delta_{\mathrm{d}}), \tag{39}$$

where the brackets denote the average over a particular sink type only.

Then the expression for the mean bias of the system can be written as

$$\bar{\delta}(k^2_{\mathrm{S}}) = \frac{k^2_{\mathrm{d}}\delta_{\mathrm{d}} + k^2_{\mathrm{C}}\langle \delta_{\mathrm{C}}(R_{\mathrm{C}}) \rangle + k^2_{\mathrm{V}} \langle \delta^{\mathrm{eff}}_{\mathrm{V}}(R_{\mathrm{V}}, k^2_{\mathrm{S}}) \rangle}{k^2_{\mathrm{d}} + k^2_{\mathrm{C}} + k^2_{\mathrm{V}}}. \tag{40}$$

Note that the bubble bias equals the mean bias of the system (Section 5.2), and hence it does not directly influence its value.

6. Simultaneous evolution of ED at high dose irradiation

Fig. 3 illustrates the radiation-induced reactions between PD and ED based on the present model. Primary radiation-induced PD, namely, H and F centers, separate ultimately into bubbles, dislocations and metal colloids, which results in the production of secondary PD (V_F centers) and ED (vacancy voids).

During the later stage of radiolysis, after the nucleation of colloids and bubbles has been completed, we have simple asymptotic equations both for their number densities Eqs. (23) and (32) and mean sizes Eq. (24) or volume fractions Eqs. (25) and (31) expressed through the steady-state dislocation density. The latter is known to saturate under irradiation (after approximately 1 dpa or 10 Grad) at some value of about 10^{14} m^{-2}, which we assume to be a fixed parameter in our calculations. The void growth rate is given by Eq. (36) while their number density depends on the rate of transition from bubbles, which we will illustrate by assuming two very different values, namely, $dN_V/dKt = 2 \times 10^{17}$ Grad^{-1} m^{-3} and 10^{21} Grad^{-1} m^{-3}. The first value for the bubble-void transition rate is deduced from a comparison with our experimental data for 300 Grad irradiation (see Section 8). The second value is more than three orders of magnitude higher, which allows forming as many voids as the bubbles can produce. And it is interesting to see (Fig. 4(b)) that the void number density in the second case is rapidly saturated below some value, N_ρ, which is determined by the dislocation density and bias and the misfit bias rather than by the void formation rate

$$N_\rho = \frac{k_d^2(\delta_d - \delta_\varepsilon)}{2\pi\alpha^{im} b}. \tag{41}$$

This is a consequence of the competition between voids and colloids that have higher bias due to misfit stress. So, as soon as the void number density reaches N_ρ, they suppress the growth of the colloid and bubble volume fractions (Fig. 5(b)), and hence the mean number of gas molecules per bubble stays just below the critical value (Fig. 6(b)) blocking further void formation. The mean colloid radius keeps growing, however (Fig. 7(b)), at the expense of the dissolution of smaller colloids due to the RIC mechanism [12]. When the radius reaches the value R_C^{th}, the colloids lose their coherency, which can strongly affect their subsequent evolution. On one hand, the misfit bias (that is due to the colloid/lattice parameter mismatch) disappears, and colloids can start growing much faster, as illustrated in Fig. 7(b). Their number density is saturated subsequently at a new asymptotic value (Fig. 4(b)) while the volume fraction increases with increasing irradiation dose. On the other hand, incoherent colloids can trap both F and V_F centers, a subsequent recombination of which would produce stoichiometric vacancy pairs, while the net colloid growth may be decreased [9]. In any case, this transition is expected to take place after a very high irradiation dose (Fig. 7(b)) which has not yet been reached in a controlled experiment. So this question needs further experimental and theoretical investigations.

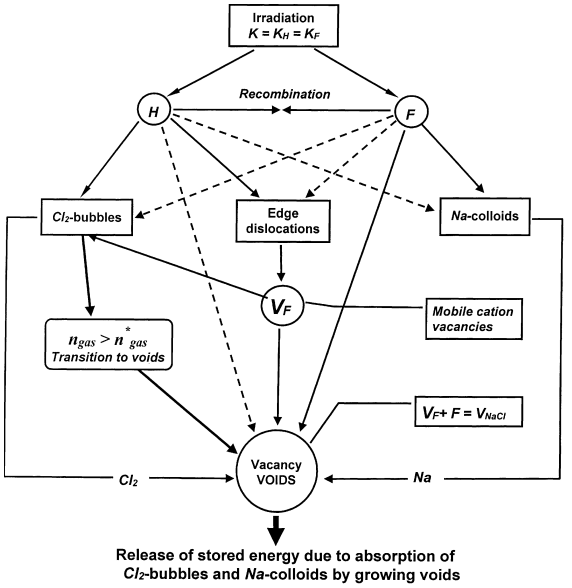

Fig. 3. Diagram of radiation-induced reactions between point defects. (H- and F-centers, and cation vacancies) and extended defects (bubbles, dislocations and colloids) resulting in the void formation.

The evolution of the system in the case of a low bubble-void transition rate is less dramatic (Figs. 4(a)–7(a)). The void influence on the mean system bias is weaker due to their low number density (Fig. 4(a)), but their radius growth rate is much faster (Fig. 7(a)). Consequently, for doses higher than 100 Grad, the void dimensions exceed the mean distance between colloids and bubbles, (R_{expl} in Fig. 8(a)), which makes possible the capture of the latter by growing voids that would eventually bring the halogen gas and metal to a back reaction inside the voids.

7. Temperature dependence of the damage production

The temperature dependence of the colloid evolution is governed by two parameters, namely, the migration and formation energies of F centers. The former determines bulk recombination of F and H centers, which

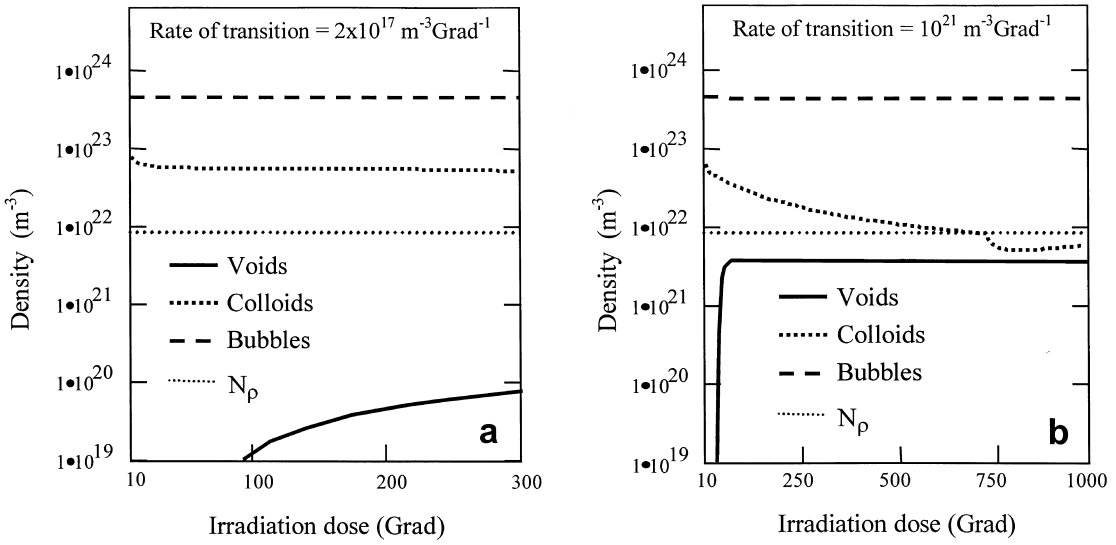

Fig. 4. Dose dependence of the number densities of extended defects for $K = K_I = 240$ Mrad/h, and $T = 100$°C. The initial decrease of the colloid number density is due to the RIC mechanism [12] adjusting N_C to its asymptotic value (Fig. 4(a)), which changes after the loss of coherency resulting in another fall down of N_C (Fig. 4(b)).

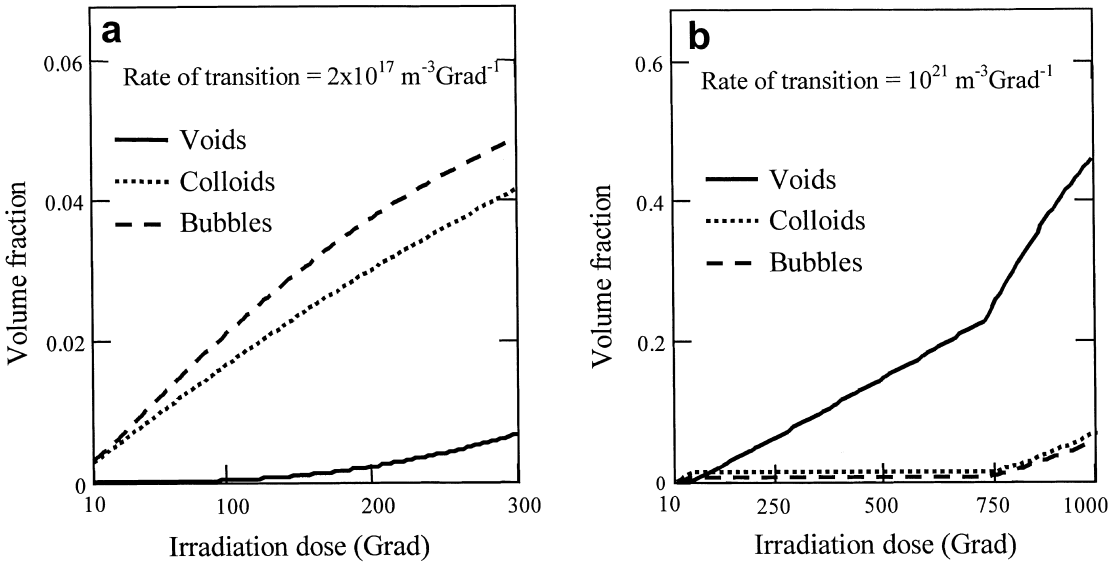

Fig. 5. Dose dependence of the volume fraction of extended defects for $K = K_I$, and $T = 100$°C. Saturation of the coherent colloid volume fraction with the dose (Fig. 5(b)) is due to the competition with voids having lower bias (no misfit stress). After the loss of coherency, the growth of the colloid volume fraction recommences. The void volume fraction grows rapidly in both regimes.

influences the product $D_H\bar{c}_H$ that enters all the growth rate expressions as a common factor. This factor increases with increasing temperature until the bulk recombination becomes negligible as compared to recombination at ED. The formation energy determines production of thermal F centers, which rapidly increases with increasing temperature and must be taken into account at high temperatures (or low dose rates) of irradiation. As it has been shown for irradiated metals [10], an account of thermal F centers results in effective increase of the colloid bias factor parameter $\alpha^{im}, \alpha_c^{im}$ by the value $(2\gamma\omega/kT)\left(D_F c_F^{(e)}/D_H\bar{c}_H\right)$, where $c_F^{(e)} = \exp\left(-E_F^f/kT\right)$ is the thermal equilibrium concentration of F center and γ is the surface energy of a particular

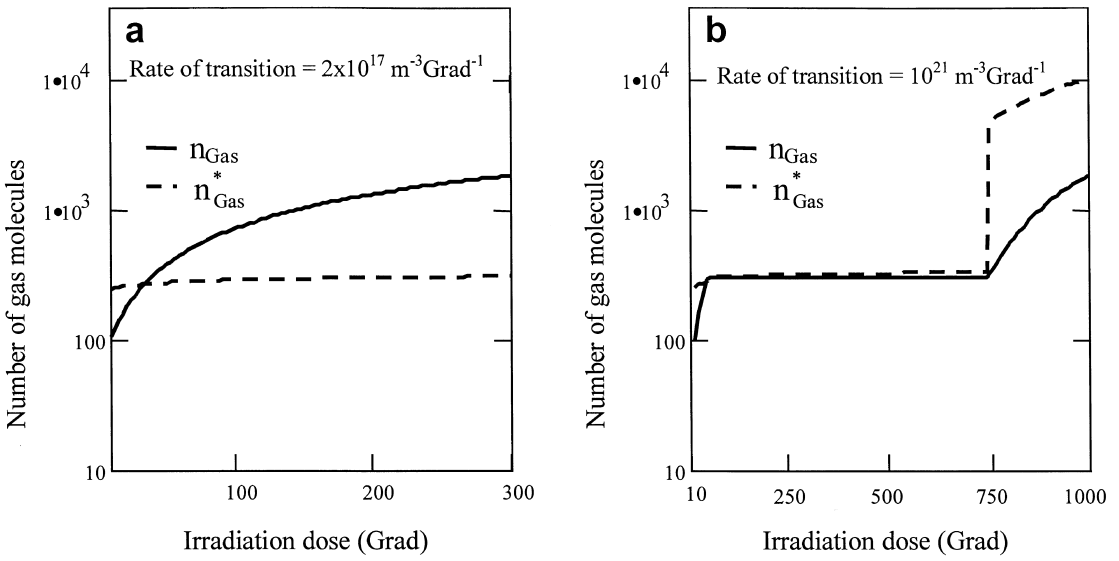

Fig. 6. Dose dependence of the mean number n_{Gas} of gas molecules in a bubble at $K = K_1$, and $T = 100°C$. n^*_{Gas} is the critical number of gas molecules for the bubble-void transition. If the bubble-void transition rate is low (Fig. 6(a)), it determines the void number density since n_{Gas} is not influenced by the voids. At high bubble-void transition rate (Fig. 6(b)), they suppress the growth of colloid and bubble volume fractions (Fig. 5(b)) keeping the mean number of gas molecule per bubble just below the critical value (Fig. 6(b)) blocking further void formation (Fig. 4(b)).

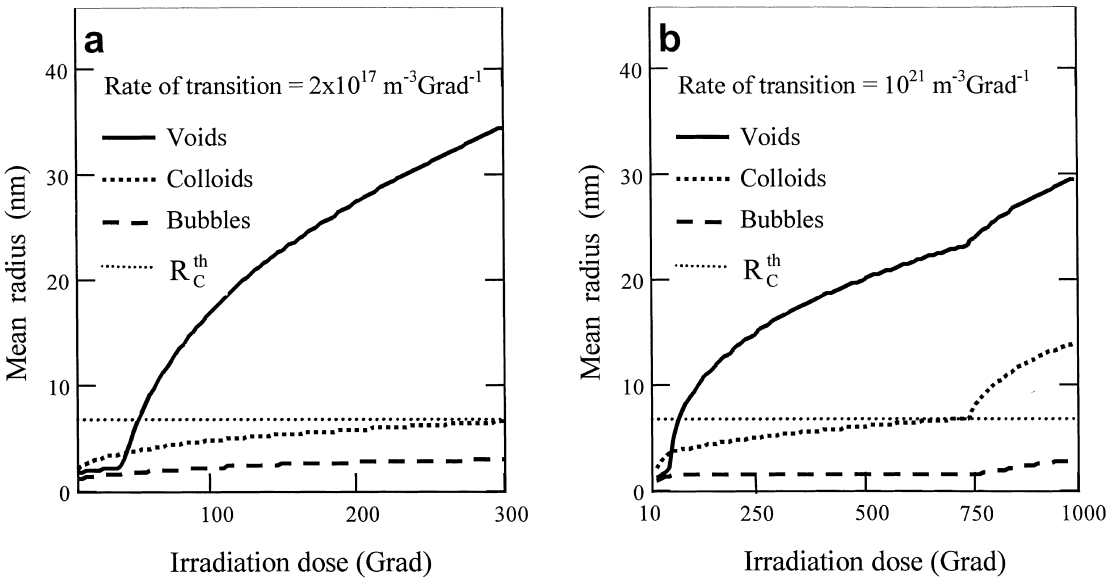

Fig. 7. Dose dependence of the mean radii of extended defects for $K = K_1$, and $T = 100°C$. (a) Very rapid void growth that does not affect the growth rates of colloids and bubbles due to a low number density of voids (Fig. 4(a)). (b) Colloid mean radius continues growing even at the constant volume fraction (Fig. 5(b)) due to the RIC mechanism. After the loss of coherency, colloid mean radius growth enhances due to the loss of misfit stress.

ED. The colloid fraction growth rate can be shown to be proportional to the difference $D_H\bar{c}_H - D_F c_F^{(e)}$, which increases with temperature in the region of bulk recombination and decreases in the region of thermal PD domination. In the intermediate region, where both bulk recombination of PD and their thermal production are negligible, the growth rate per dpa reaches its maximum value, which is independent on the temperature and dose

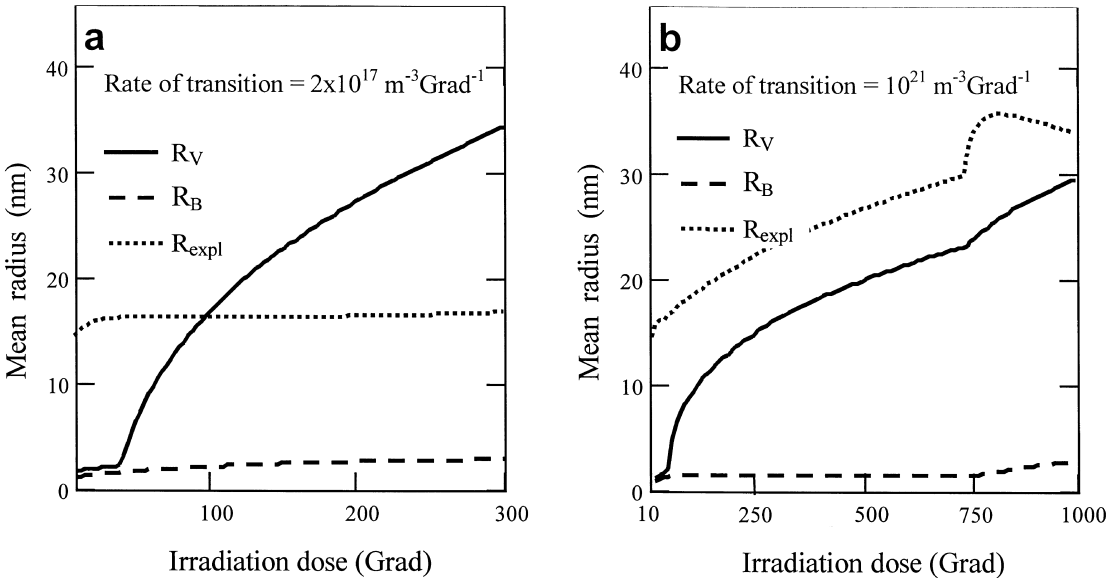

Fig. 8. Dose dependence of the mean radii of extended defects and the mean distance between colloids and bubbles, R_{expl}, $K = K_1$, $T = 100°C$. At $R_V > R_{exp}$, colloids and bubbles start to be captured by growing voids, which would eventually bring the halogen gas and metal to a back reaction inside the voids.

rate and is determined only by the sink strengths (the same is true for the void swelling rate in metals [10–12]). The result is shown in Fig. 9 both for our dose rate and for that assumed to model the nuclear waste repository irradiation. In both cases, we can see the usual bell shape temperature dependence shifting along the temperature axis with changing dose rate. The dose required for F centers (the slowest PD in the system) to reach a steady state determines the lower cut-off temperature of colloid formation. The upper cut-off temperature is determined by the sum of the F center migration and formation energies.

The expressions for critical parameters (33) and (34) remain unchanged but the form of the effective parameters γ_K and σ_K will be different due to the account of thermal PD [10,22]

$$\gamma_K = \gamma + \mu b \frac{\alpha^{im}}{2\alpha_K^d}, \quad \sigma_K = \mu \frac{\bar{\delta}}{\alpha_K^d},$$
$$\alpha_K^d \equiv \alpha^d + \frac{D_F c_F^{(e)}}{D_H \bar{c}_H} \frac{\omega\mu}{kT}. \tag{42}$$

The voids are thermally more stable as compared to colloids since their dissolution is determined by the sum of the F and V_F center migration and formation energies. Accordingly, the annealing behavior of irradiated NaCl after irradiation can be understood as the dissolution of colloids at moderate temperatures (between 250°C and 400°C [23]). This results in a back reaction of liberated F centers ('evaporated' excess Na from the colloids) with halogen molecules in bubbles, which leaves behind

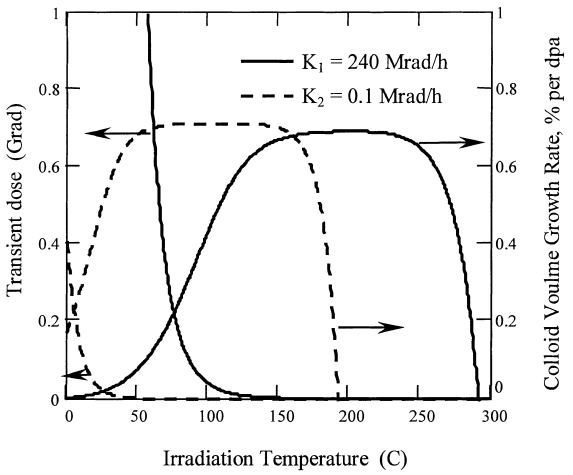

Fig. 9. Temperature dependence of the radiation damage production. Colloid volume growth rate at different dose rates, corresponding to the laboratory irradiation (K_1) and irradiation in the nuclear waste repository (K_2). The left curves show temperature dependence of the dose required for F centers (the slowest PD in the system) to reach a steady state, which determines the lower cut-off temperature of colloid formation. The upper temperature cutoff is determined by the sum of the F center formation and migration energies.

vacancy voids and dislocations that could be annealed only at higher temperatures (above 400–450°C [23]). So a moderately annealed crystal still persists in showing a lower density (i.e., a volume expansion) than an unirradiated crystal up to 400°C. We predict with this model

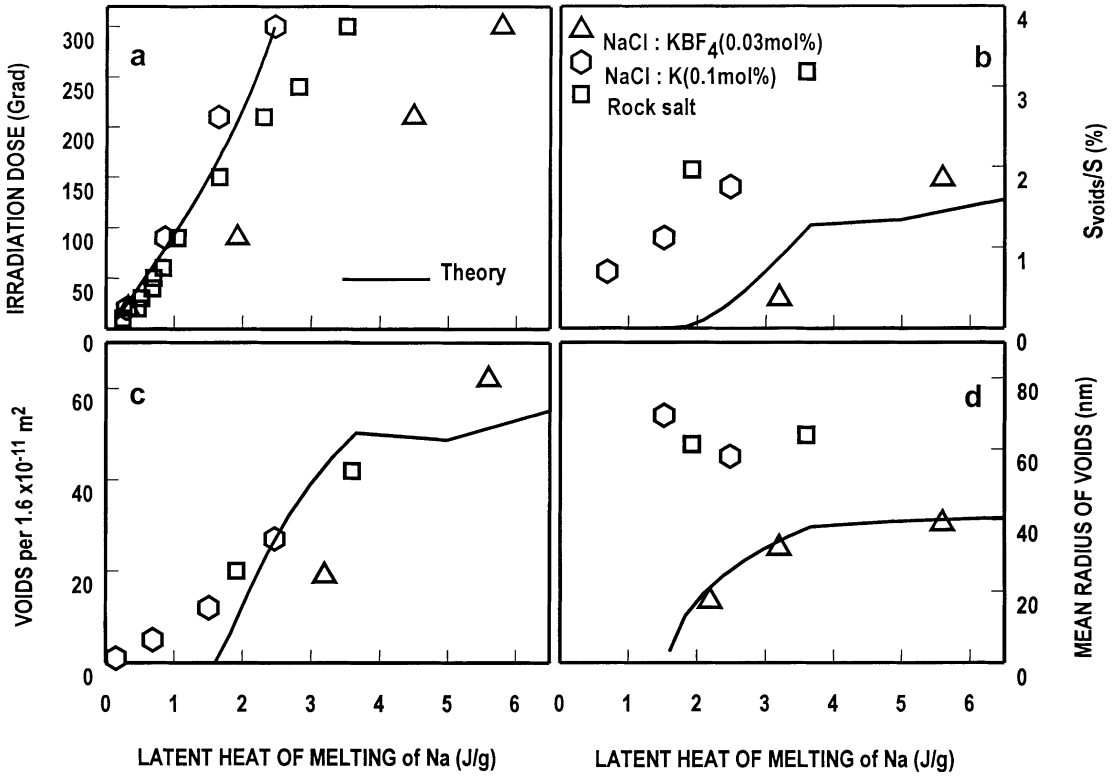

Fig. 10. Comparison between experiment [6,7] and the present theory. (a) Measured and calculated dependence of LHM of metallic Na, which is proportional to the colloid fraction, on irradiation dose ($K = K_1$) at 100°C. (b)–(d) Void mean parameters (volume fraction (b), number density (c) and mean radius (d)) against LHM measured after irradiation up to 300 Grad (symbols) for different dopants and temperatures (from 60°C to 130°C) and calculated (curves) assuming $K = K_1$, dislocation density $\rho_d = 10^{14}$ m^{-2}, and the void formation rate $dN_V/dKt = 2 \times 10^{17}$ Grad^{-1} m^{-3}.

that a subsequent irradiation of this, not fully recovered crystal, at lower temperatures may result in further void development instead of colloid formation that would be suppressed by voids. Such a result can be expected, however, after sufficiently long irradiation to produce halogen bubbles with sizes exceeding the critical void size, which corresponds to the critical number of vacancy pairs, n_{Vcrit}, in Fig. 3. Below this size, empty voids formed as a result of annealing would have a larger bias for H centers than that of dislocations. Such voids would be filled with halogen under the subsequent irradiation and provide an additional driving force for the colloid growth instead of suppressing it.

The critical void size is determined by the ratio of its bias constant to the dislocation bias to be about 1.7 nm. The mean bubble size can reach this value after irradiation dose of about 50 Grad (which is even higher than the dose 40 Grad required for the bubble-void transition onset). So the annealing up to 400°C should enhance (or suppress) the colloid production under a subsequent irradiation if the initial dose were lower (or higher) than 50 Grad. The former conclusion agrees with experimental data by Hodgson et al. [23] who observed that such a treatment enhanced the colloid production after initial irradiation up to 5 Grad and suggested that vacancy pairs and/or their clusters were responsible for colloid nucleation. Experimental data on the effect of annealing after higher irradiation doses do not exist to our knowledge.

8. Discussion of the results and comparison with experimental data

The present theory is based on a new mechanism of dislocation climb, which involves the production of V_F centers (self-trapped hole neighboring a cation vacancy) as a result of the absorption of H centers. There exist a lot of experimental data on cation vacancy production in alkali halides under irradiation (see, e.g. [23,24]) and on the formation of vacancy pairs and their small aggregates [25].

Based on the model presented in this paper, a complete set of the rate equations for PD and growth rates for ED was derived in Section 7. An asymptotic (in time of irradiation) solution to these equations was obtained in the temperature range, in which both anion

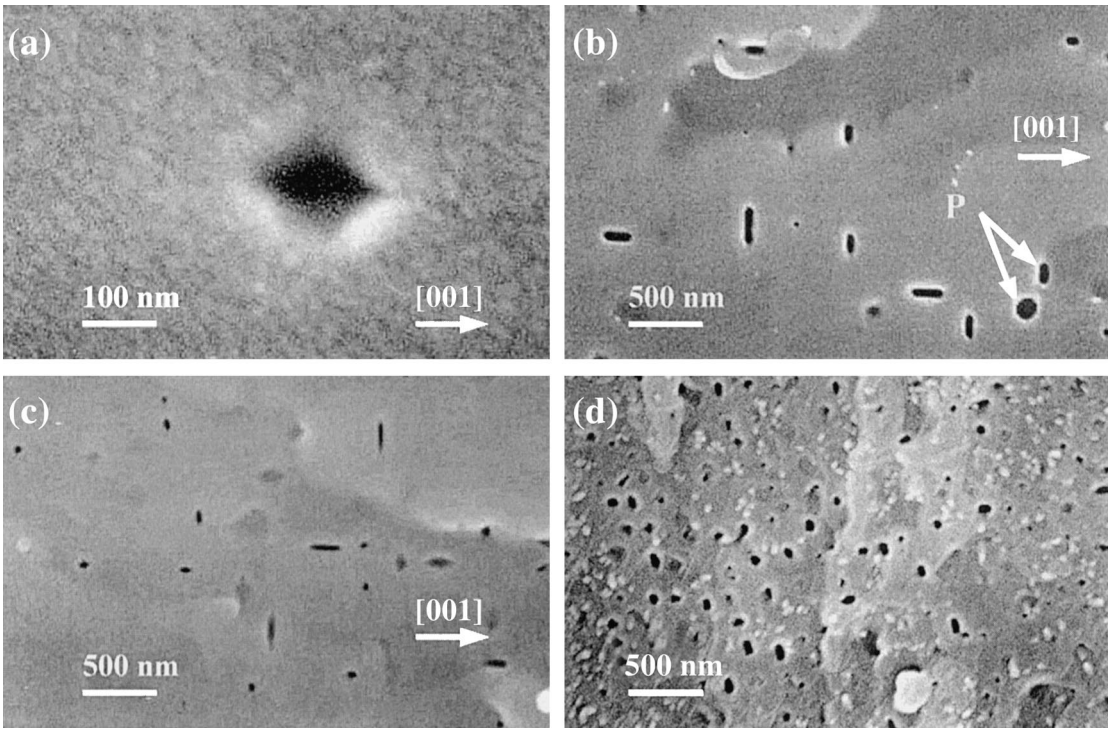

Fig. 11. SEM micrographs showing vacancy voids in doped and natural NaCl samples irradiated with 0.5 MeV electrons to a dose of 300 Grad. (a) Equiaxial void at high resolution in natural rock salt irradiated up to 60 Grad; latent heat of melting (LHM) of metallic Na is 0.45 J/g. (b) 'Penny-shaped' voids/cracks in natural rock salt irradiated up to 300 Grad; LHM of metallic Na is 2 J/g. Two adjacent voids with different orientations are shown by the arrows. (c) Penny-shaped voids/cracks in NaCl + K (0.1 mol%) irradiated up to 90 Grad; LHM of metallic Na is 1.7 J/g. (d) Equiaxial voids in NaCl + KBF_4 (0.03 mol%) irradiated at 100°C up to 300 Grad; LHM of metallic Na is 5.6 J/g.

and cation PD are mobile. In this region, the growth or shrinkage rates of different kinds of ED and their sizes are determined by the difference between the incoming fluxes of radiation-induced PD, which is determined by several material constants presented in Table 1. We have used a typical value for the mean dislocation density, $\rho_d = 10^{14}$ m^{-2} and two values for the void formation rate, $dN_V/dKt = 2 \times 10^{17}$ Grad^{-1} m^{-3} and 10^{21} Grad^{-1} m^{-3}, as the only input microstructural parameters. The first value for the void formation rate has been deduced from a comparison with the observed void number density of about 10^{20} m^{-3} after 300 Grad irradiation[2] [6–8]. To make a quantitative comparison of the other calculated ED parameters with experimental data we have to take into account that they have been obtained at different temperatures ranging from 60°C to 130°C. In this range, as can be seen from Fig. 9, the temperature dependence of ED evolution is due to F center increasing mobility since their thermal production is negligibly small as compared to that by irradiation.

Fig. 10(a) shows the calculated and measured dose dependencies of the sodium latent heat of melting (LHM) at 100°C. LHM is proportional to the colloid volume fraction, which can be seen to correlate with void parameters in Fig. 10(b)–(d) measured at temperatures ranging from 60°C to 130°C. The experimental data for voids in NaCl doped with KBF_4 (illustrated also in Fig. 11(a)) seem to be in agreement with the calculations done assuming the experimentally observed void formation rate. In this case, there is no saturation of colloid growth, and besides, for doses higher than 100 Grad, the void dimensions may exceed the mean distance, first, between bubbles and then between colloids (R_{expl} in Fig. 8(a)) resulting in their collisions with voids. Collisions with bubbles fill the voids with gas, and subsequent collisions with colloids bring the halogen gas and metal to a back reaction inside the voids. Such a sudden release of stored energy

[2] In this paper we have used a new code for the dose rate calculation, which gives a total dose reached in our experiments about 300 Grad instead of 150 Grad assumed in [6–8]. This difference is due to the beam reflection from the sample holders, which is taken into account by the new code.

can be shown to result in a drastic rise of temperature (above 10^4 K) and gas pressure (up to 1 GPa) within voids [26], which may transform equiaxial voids into penny shaped cracks along the cleavage planes in the matrix, as it is demonstrated in Fig. 11(a) and (b). Fig. 11(b) and (c) show penny shaped voids/cracks in natural rock salt samples and in NaCl doped with K as compared to equiaxial voids formed in heavily irradiated NaCl doped with KBF_4 (Fig. 11(d)). Obviously, the dimensions of penny shaped voids should be larger than those calculated in the framework of diffusion void growth mechanism. This explains the discrepancy between theoretical curves and experimental data and shows the need for a new (explosion driven) mechanism of void/crack growth in irradiated NaCl resulting in a subsequent material destruction, which has been observed in some of our samples [6,7] The effect of particular dopants on the void-crack transition dose needs further investigation.

The presented scenario of the evolution of radiation-induced stored energy in rock salt is in a marked contrast with that predicted by previous models reviewed by Soppe et al. [27]. The main conclusion there was a *saturation* of the stored energy with increasing irradiation dose due to a back reaction between F centers and dispersed molecular centers as was proposed originally by Lidiard [28]. But, first, the model of dispersed molecular centers is in a contradiction with recent observations of large voids [6,7], as well as with early observations of halogen bubbles after a high dose irradiation [29]. Second, assuming the model of dispersed molecular centers, it is hard to expect a high activation barrier for their recombination with F centers since the energy liberated during the recombination appears to be about 5 eV for NaCl [1]. Such a barrier (0.6 eV), has been assumed, however, to reconcile the model with the experiments by Jenks and Bopp (see Refs. in [27]), which did show a saturation behavior of colloid fraction at high doses.[3] This saturation, however, can be naturally explained by the present model to be a consequence of the competition with voids when their number density is high enough (see Section 6). What is important is that the saturation of colloid fraction does not mean a saturation of radiation damage, which is also evident from Fig. 5(b). From a practical point of view, that means a swelling of the salt comparable to that observed in irradiated metals. Fig. 12 illustrates this conclusion further by presenting fractions of colloids and voids after irradiation to 200 Grad at different dislocation and bubble densities in the case of unrestricted bubble-void

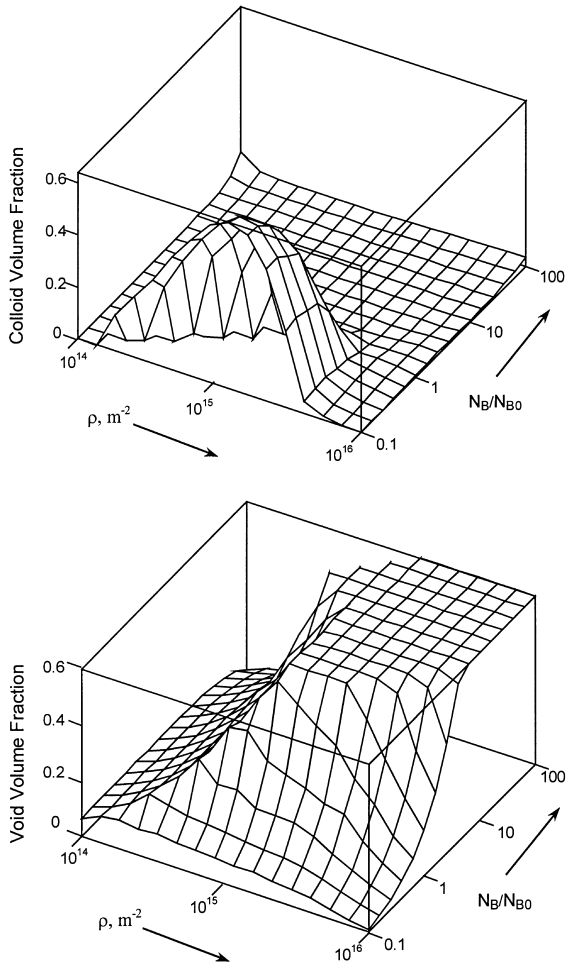

Fig. 12. Volume fractions of colloids and voids after irradiation to 200 Grad for different dislocation and bubble densities. The latter is presented as the ratio N_B/N_B^0, where N_B^0 is given by Eq. (32), $dN_V/dKt = 10^{21}$ Grad^{-1} m^{-3}.

transition. One can see that in the region where both dislocation and bubble densities are high, the colloid fraction is suppressed but the void fraction is higher than 50%. Obviously, this can lead to a serious deterioration of the integrity of the repository as well as the back reaction of colloids and bubbles.

The present results should not be regarded as predictions of the rock salt behavior in the real conditions of depository. We still need to know more about material parameters controlling transitions between the different regimes of radiolysis. And certainly more experimental data on material response to super high irradiation doses are required in order to make definite conclusions. At the present stage, we would like to conclude that the amount of radiation damage in alkali halides could not be evaluated correctly without account of vacancy void and crack formation.

[3] It should be noted that systematic experiments on many (pure, doped and natural rock salt) heavily irradiated samples have shown that with increasing dose the stored energy value increases without any sign of saturation [30].

9. Summary

1. A new mechanism of dislocation climb under irradiation of alkali halides is presented, which involves production of V_F centers as a result of absorption of extra H centers.
2. The difference between the bias factors of extended defects of different kinds or sizes is shown to be the main driving force of the radiolysis at elevated temperatures.
3. Voids are shown to arise from halogen bubbles due to agglomeration of F and V_F centers at their surfaces. Critical values for the bubble-void transition are evaluated.
4. Mean sizes and volume fractions of all defect types at the late stage of radiolysis are calculated and compared with experimental data for NaCl.
5. Voids can grow to the dimensions exceeding the mean distance between colloids and bubbles, eventually absorbing them, and, hence, bringing the halogen gas and metal to a back reaction.
6. The amount of radiation damage in alkali halides should be evaluated with account of vacancy void formation, which strongly affects the radiation stability of material.

Acknowledgements

This study is supported by the Dutch Ministry of Economic Affairs.

References

[1] A.B. Lidiard, Comments Solid State Phys. 8 (1978) 73.
[2] L.W. Hobbs, A.E. Huges, Pooley, Proc Roy. Soc. London A332 (1973) 167.
[3] Uma Jain, A.B. Lidiard, Philos. Mag. 35 (1977) 245.
[4] A.E. Hughes, Comments Solid State Phys. 8 (1978) 83.
[5] V.N. Kuzovkov, E.A. Kotomin, W. von Niessen, Phys. Rev. B (1998) 8454.
[6] D.I. Vainshtein, C. Altena, H.W. Den Hartog, Mater. Sci. Forum 607 (1997) 239.
[7] H.W. Den Hartog, D.I. Vainshtein, Mater. Sci. Forum 611 (1997) 239.
[8] D.I. Vainshtein, V.I. Dubinko, A.A. Turkin, H.W. den Hartog, Void formation in heavily irradiated NaCl, Presented at EURODIM'98 Keele, 1998.
[9] V.I. Dubinko, A.A. Turkin, D.I. Vainshtein, H.W. den Hartog, New formulation of the modeling of radiation-induced microstructure evolution in alkali halides, Presented at EURODIM'98 Keele, 1998.
[10] V.I. Dubinko, J. Nucl. Mater. 206 (1993) 1.
[11] V.I. Dubinko, J. Nucl. Mater. 225 (1995) 26.
[12] V.I. Dubinko, P.N. Ostapchuk, V.V. Slezov, J. Nucl. Mater. 161 (1989) 239.
[13] W.G. Wolfer, M. Ashkin, J. Appl. Phys. 46 (1975) 547.
[14] P.N. Ostapchuk, N.I. Ischenko, On the void bias factor in elastically anisotropic cubic crystals, Preprint KIPT 93-19, Kharkov 1993, p. 14.
[15] E.J. Savino, Philos. Mag. 36 (1977) 323.
[16] P.H. Dederich, K. Schroeder, Phys. Rev. B 17 (1978) 2524.
[17] V.A. Borodin, A.I. Ryazanov, C. Abromeit, J. Nucl. Mater. 207 (1993) 242.
[18] G.W. Greenwood, A.J.E. Foreman, D.E. Rimmer, J. Nucl. Mater. 4 (1959) 305.
[19] J.H. Evans, A. VanVeen, L.M. Caspers, Radiat. Eff. 78 (1983) 611.
[20] V.I. Dubinko, V.V. Slezov, A.V. Tur, V.V. Yanovskij, Radiat. Eff. 100 (1986) 85.
[21] L.K. Mansur, E.H. Lee, P.J. Maziasz, A.P. Rowcliffe, J. Nucl. Mater. 633 (1986) 141.
[22] V.I. Dubinko, J. Nucl. Mater. 832 (1996) 233.
[23] E.R. Hodgson, A. Delgado, F. Agullo-Lopez, F.J. Lopez, Radiat. Eff. 74 (1983) 193.
[24] Ch. Lushchik, N. Lushchik, A. Frorip, O. Nikiforova, Phys. Stat. Sol. b 168 (1991) 413.
[25] A.V. Gektin, V. Ya Serebryany, N.V. Shiran, Radiat. Eff. Def. Sol. 134 (1995) 411.
[26] D.I. Vainshtein, V.I. Dubinko, A.A. Turkin, H.W. den Hartog, Effect of the void size distribution on the explosive decomposition of electron irradiated NaCl crystals, submitted to the 10th International Conference on Radiation Effects in Insulators (REI-10), 18–23 July 1999, Jena, Germany.
[27] W.J. Soppe, H. Donker, A. Garcia Celma, J. Prij, J. Nucl. Mater. 217 (1994) 1.
[28] A.B. Lidiard, Philos. Mag. 39 (1979) 647.
[29] L.W. Hobbs, A.E. Hughes, Radiation damage in diatomic materials at high doses, Harwell Report AERE–R 8092, 1975.
[30] H.W. Den Hartog, J.C. Groote, J.R.W. Weerkamp, Radiat. Eff. Def. Sol. 139 (1996) 1.